DMD Fast Forward. Published on June 14, 2022 as DOI: 10.1124/dmd.122.000930
This article has not been copyedited and formatted. The final version may differ from this version.

DMD-AR-2022-000930

Title

Cytochrome P450 2J (CYP2J) Genes in Dogs, Cats, and Pigs Are Expressed and Encode Functional Drug-Metabolizing Enzymes

Yasuhiro Uno[a,*], Norie Murayama[b], Moe Ijiri[a], Hiroaki Kawaguchi[c], Osamu Yamato[a], Mitsuya Shiraishi[a], Atsushi Asano[a], Hiroki Teraoka[d], Hazuki Mizukawa[e,f], Shouta M.M. Nakayama[e], Yoshinori Ikenaka[e], Mayumi Ishizuka[e], and Hiroshi Yamazaki[b,*]

[a] Joint Faculty of Veterinary Medicine, Kagoshima University, Kagoshima 890-8580, Japan

[b] Showa Pharmaceutical University, Machida, Tokyo 194-8543, Japan

[c] School of Veterinary Medicine, Kitasato University, Towadashi, Aomori 034-8628, Japan

[d] School of Veterinary Medicine, Rakuno Gakuen University, Ebetsu, Hokkaido 069-8501, Japan

[e] Graduate School of Veterinary Medicine, Hokkaido University, Sapporo 060-0818, Japan

[f] Graduate School of Agriculture, Ehime University, Matsuyama, Ehime 790-8566, Japan

Running title: New Dog, Cat, and Pig P450 2J Enzymes

* All correspondence should be sent to**:**

1) Yasuhiro Uno, D.V.M., Ph.D.
Joint Faculty of Veterinary Medicine, Kagoshima University, 1-21-24 Korimoto, Kagoshima-city, Kagoshima 890-8580, Japan
Phone/Fax: +81-99-285-8715. E-mail address: unoxx001@vet.kagoshima-u.ac.jp

or

2) Hiroshi Yamazaki, Ph.D.
Laboratory of Drug Metabolism and Pharmacokinetics, Showa Pharmaceutical University, 3-3165 Higashi-Tamagawa Gakuen, Machida, Tokyo 194-8543, Japan
Phone: +81-42-721-1406. Fax: +81-42-721-1406. E-mail address: hyamazak@ac.shoyaku.ac.jp

Number of text pages: 26

Number of tables: 2

Number of figures: 8

Number of references: 34

Number of words in abstract: 250 words

Number of words in introduction: 430 words

Number of words in discussion: 1225 words

Abstract

Cytochromes P450 (P450 or CYP) have been identified and analyzed in dogs and pigs, species that are often used in preclinical drug studies. Moreover, P450s are clinically important for drug therapy not only in humans but also in species under veterinary care, including dogs and cats. In the present study, seven P450s homologous to human CYP2J2, namely, dog CYP2J2; cat CYP2J2; and pig CYP2J33, CYP2J34, CYP2J35, CYP2J91, and CYP2J93, were newly identified and characterized. The cDNAs of these CYP2Js contained open reading frames of 502 amino acids, except for CYP2J35 (498 amino acids), and shared high sequence identity (77–80%) with human CYP2J2. Phylogenetic analysis revealed that dog and cat CYP2J2 were closely related, whereas pig CYP2Js formed a cluster. All seven *CYP2J* genes contain nine coding exons and are located in corresponding genomic regions, with the pig *CYP2J* genes forming a gene cluster. These CYP2J2 mRNAs were predominantly expressed in small intestine with additional expression in kidney and brain for dog CYP2J2 and pig CYP2J91 mRNAs, respectively. All seven CYP2Js metabolized human CYP2J2 substrates terfenadine, ebastine, and astemizole, indicating that they are functional enzymes. Dog CYP2J2 and pig CYP2J34 and CYP2J35 efficiently catalyzed ebastine primary hydroxylation and secondary carebastine formation at low substrate concentrations, just as human CYP2J2 does. Velocity-versus-substate plots exhibited sigmoidal relationships for dog CYP2J2, cat CYP2J2, and pig CYP2J33, indicating allosteric interactions. These results suggest that dog, cat, and pig CYP2Js have similar functional characteristics to human CYP2J2, with slight differences in ebastine and astemizole oxidations.

Significance Statement

New dog cytochrome P450 2J2 (CYP2J2); cat CYP2J2; and pig CYP2J33, CYP2J34, CYP2J35, CYP2J91, and CYP2J93, homologous to human CYP2J2, were identified and characterized by sequence, phylogenetic, and genomic structure analyses. Intestinal expression patterns of CYP2J mRNAs were characteristic in dogs, cats, and pigs. Dog, cat, and pig CYP2Js likely play roles as drug-metabolizing enzymes in small intestine, similar to human CYP2J2.

Introduction

Cytochromes P450 (P450s or CYPs) are important drug-metabolizing enzymes and have been identified and analyzed in dogs and pigs, species that are often used in preclinical drug metabolism studies during drug development. P450s are clinically important for drug therapy not in only humans but also in species under veterinary care, including dogs and cats. Some P450s have been identified in dogs, cats, and pigs and show characteristics similar to those of humans, but some differences from humans have been noted. For example, dog CYP2B11, which is orthologous to human CYP2B6, is abundant in both liver and small intestine, unlike its prevalent expression in liver in humans, and metabolizes substrates such as midazolam that human CYP2B6 does not metabolize (Court, 2013). Pig CYP2B22 is homologous to human CYP2B6 but is not detected in liver at the protein level, unlike CYP2B6 in humans (Elmorsi et al., 2020). In cats, two *CYP2C* genes are present in the genome, of which one is a pseudogene and the other is expressed at low levels in liver, indicating a limited role of cat CYP2Cs in liver, unlike the situation in humans, in which CYP2Cs are the second most important group of P450 in humans after CYP3As (Ono et al., 2019). Therefore, the identification and characterization of individual P450 forms are important to understand P450-mediated drug metabolism in different species.

CYP2J2 is an important P450 in humans because it is a drug-metabolizing enzyme involved in the first-pass metabolism of ebastine and astemizole (Hashizume et al., 2002; Matsumoto et al., 2002). Human CYP2J2 also metabolizes numerous substrates of human CYP3A4 because of the large volume of its active site (Lee et al., 2010); this fact increases the importance of CYP2J2 for drug metabolism. In humans, CYP2J2 is expressed in various tissues, including liver and small intestine, and is abundant in cardiac tissues such as heart muscle (Wu et al., 1996; Zeldin et al., 1997; Delozier et al., 2007). CYP2J2 plays roles in the metabolism of not only drugs but also endogenous substrates such as arachidonic acid, thereby generating epoxyeicosatrienoic acids that are important for their protective roles in inflammation and vasodilation (Xu et al., 2013; Murray, 2016; Solanki et al., 2018). Despite the importance of CYP2J enzymes, to date, CYP2Js have not been identified and

characterized in pigs, dogs, or cats.

In the present study, the following cDNAs homologous to human CYP2J2 were identified in dogs, cats, and pigs: dog CYP2J2; cat CYP2J2; and pig CYP2J33, CYP2J34, CYP2J35, CYP2J91, and CYP2J93. These CYP2Js were characterized by sequence and phylogenetic analyses, genomic structures, tissue expression patterns, and metabolic assays.

Materials and Methods

Materials

Astemizole, terfenadine, and terfenadine alcohol were purchased from Sigma-Aldrich (St. Louis, MO); desmethylastemizole was purchased from Toronto Research Chemicals (Toronto, Canada); and ebastine, hydroxyebastine, and carebastine were purchased from Almirall-Prodesfarma (Barcelona, Spain). Pooled liver microsomes from dogs and humans were purchased from Corning Life Sciences (Woburn, MA). Oligonucleotides were synthesized by Integrated DNA Technologies (Coralville, IA). All other reagents were purchased from Sigma-Aldrich or Fujifilm Wako Pure Chemicals (Osaka, Japan), unless otherwise specified.

Tissues and Nucleic Acid Preparation

Samples of adrenal gland, heart, ileum, jejunum, kidney, liver, and lung were collected from a beagle dog (male, 2 years of age, weighing 10 kg) at Shin Nippon Biomedical Laboratories, Ltd. (Kainan, Japan), a cat (male, 23 months of age, weighing 4.73 kg) at Hokkaido University, and a pig (female, 10 years of age, weighing 13 kg) at Kagoshima University. Additional tissues were collected from the same animals, i.e., brain and testis from the dog; duodenum, spleen, and testis from the cat; and brain, ovary, and uterus from the pig. Moreover, a liver sample was also collected from a cat (female, 6 months of age, unknown weight) at Kagoshima University and used for molecular cloning. Total RNAs were extracted from dog tissues using a mirVana miRNA isolation kit (Ambion, Austin, TX) and from cat and pig tissues using an RNeasy Mini Kit (Qiagen, Valencia, CA) from cat and pig tissues, according to the manufacturers' protocols. Cat and pig liver microsomes were prepared as described previously (Uehara et al., 2014; Uehara et al., 2015). This study was reviewed and approved by the Institutional Animal Care and Use Committee at Kagoshima University.

Molecular Cloning

Reverse transcription (RT)-polymerase chain reaction (PCR) was performed using total RNA

extracted from cat, dog, and pig liver and from pig small intestine as described previously (Uno et al., 2006). The primers were designed using Primer3 v.0.4.0 (https://primer3.ut.ee/). Briefly, first-strand cDNA synthesis was carried out in a reaction mixture containing 1 μg of total RNA, oligo (dT), and ReverTra Ace (TOYOBO, Osaka, Japan) at 42°C for 1 h according to the manufacturer's protocols. PCR reactions were performed using the RT product as the template with Q5 Hot Start High-Fidelity DNA Polymerase (New England BioLabs, Ipswich, MA) and a T100 thermal cycler (Bio-Rad Laboratories, Hercules, CA) according to the manufacturer's protocols. The PCR conditions were initial denaturation at 98°C for 30 s; followed by 35 cycles of 98°C for 10 s, 60°C for 20 s, and 72°C for 50 s; followed by a final extension at 72°C for 2 min. The primers used were dCYP2J2 (5rt1) 5′-CAGCAGAGCGAGAGGACGCGAGA-3′ and dCYP2J2 (3rt1) 5′-CCGTATTCTCAGAGGACACACCAATTCTTC-3′ for dog CYP2J2, fCYP2J2 (5rt1) 5′-CTCAGCCGAGCGAGAGGACTTTG-3′ and fCYP2J2 (3rt1) 5′-CTTCAAGACCGAGGGACTGCACAGA-3′ for cat CYP2J2, pCYP2J33 (5rt1) 5′-GAACACGGAAGAGCGGGACACT-3′ and pCYP2J33 (3rt1) 5′-GAACACGGAAGAGCGGGACACT-3′ for pig CYP2J33, pCYP2J34 (5rt1) 5′-GTCTTTGGCTCAAACCGCAGAACT-3′ and pCYP2J34 (3rt1) 5′-GGACCATACTAATCTTCTCTGTATCGTTCCAAT-3′ for pig CYP2J34, pCYP2J35 (5rt1) 5′-GGAAGAGCAGGCGGATGTCTCA-3′ and pCYP2J35 (3rt1) 5′-CCAAACCAGTTAAAGTCTTTTATTTCTCCTGAT-3′ for pig CYP2J35, pCYP2J2L (5rt1) 5′-CCGCGGAAGAGCAAGCGTA-3′ and pCYP2J2L (3rt1) 5′-GGTTTCCAAACCACTTCAAGTCCA-3′ for pig CYP2J91, and pCYP2J93 (5rt1) 5′-AGATCTCCGAAGAGCTGGAGGCTA-3′ and pCYP2J93 (3rt1) 5′-CCAAACCAGTTAAAGTCTTTTATTTCTCCCAAT-3′ for pig CYP2J93. The amplified products were cloned into pMiniT2.0 vectors using a PCR Cloning Kit (New England BioLabs) according to the manufacturer's protocol. The inserts were sequenced using an ABI PRISM BigDye Terminator v3.0 Ready Reaction Cycle Sequencing Kit (Applied Biosystems, Foster City, CA) with an ABI

DMD Fast Forward. Published on June 14, 2022 as DOI: 10.1124/dmd.122.000930
This article has not been copyedited and formatted. The final version may differ from this version.

PRISM 3500xl Genetic Analyzer (Applied Biosystems).

Bioinformatics

Sequence data were analyzed using the Genetyx system (Software Development, Tokyo, Japan), including the ClustalW program, which was used for multiple alignment of amino acid sequences. A phylogenetic tree was created by the neighbor-joining method. BLAST (National Center for Biotechnology Information) was used for the homology search, and BLAT (UCSC Genome Bioinformatics) and Sequence Viewer (National Center for Biotechnology Information) were used for analysis of the dog, cat, pig, and human genome data. Amino acid and cDNA sequences used for the analyses were from GenBank or the present study.

Quantification of mRNA Expression

Expression levels of CYP2J mRNAs were measured using real-time RT-PCR, as reported previously (Uno et al., 2006), with gene-specific primers in pig adrenal gland, brain, heart, ileum, jejunum, kidney, liver, lung, ovary, and uterus; in dog adrenal gland, brain, heart, ileum, jejunum, kidney, liver, lung, and testis; and in cat adrenal gland, duodenum, heart, ileum, jejunum, kidney, liver, lung, spleen, and testis. Briefly, RT reactions were carried out using a ReverTra Ace qPCR RT kit (TOYOBO) according to the manufacturer's protocols, and one-twentieth of the reaction mixture was subsequently used for PCR. The PCR amplification was conducted in a total volume of 20 μl using a THUNDERBIRD SYBR qPCR Mix Kit (TOYOBO) and a StepOnePlus Real-Time PCR System (Applied Biosystems), following the manufacturers' protocols. The following primers were used at final concentrations of 300 nM: d&fCYP2J2 (5qrt1) 5′-CAACTTCTTCCATCTGGACTTTGA-3′ and d&fCYP2J2 (3qrt1) 5′- TTGATCAAGGGCAATCCAGTTA-3′ for dog and cat CYP2J2, pCYP2J33 (5qrt1) 5′-GCTGGAACTGACACAACTTTGATAAC-3′ and pCYP2J33 (3qrt1) 5′-CTTGGACTTTTTCTTGGATTTCG-3′ for pig CYP2J33, pCYP2J34 (5qrt1) 5′-GTGCAGGTCCAGCTCTACAATATG-3′ and pCYP2J34 (3qrt1) 5′-TTTCAATCACACAGGCAACAAAT-3′ for pig CYP2J34, pCYP2J35 (5qrt1)

DMD Fast Forward. Published on June 14, 2022 as DOI: 10.1124/dmd.122.000930
This article has not been copyedited and formatted. The final version may differ from this version.

5′-CCCCACCAAATCATCTTTAGTAACA-3′ and pCYP2J35 (3qrt1) 5′-TGAAGGTGAACTGCCCTTTTCTA-3′ for pig CYP2J35, pCYP2J2L (5qrt1) 5′-ATCAACGCAATGCCAGTTCTA-3′ and pCYP2J2L (3qrt1) 5′-TCTGTCCTGTGATTTTCAATCATTC-3′ for pig CYP2J91, and pCYP2J93 (5qrt1) 5′-GCTCCATCACATTTGGAGAAC-3′ and pCYP2J93 (3qrt1) 5′-GATATTGTAAATCTGGCACCACAC-3′ for pig CYP2J93. Relative expression levels were determined, based on three independent amplifications, by normalization of the raw data with the 18S ribosomal RNA levels, which were measured using TaqMan Gene Expression Assays (Assay ID: Hs99999901_s1, Applied Biosystems) with THUNDERBIRD Probe qPCR Mix (TOYOBO).

Heterologous Protein Expression

Expression plasmids were generated with the CYP2J cDNAs isolated in the present study, followed by protein expression in *Escherichia coli*, as reported previously (Iwata et al., 1998; Uno et al., 2006). To enhance protein expression, the *N*-terminus was modified by PCR-amplification of the coding region using Q5 Hot Start High-Fidelity DNA Polymerase (New England BioLabs) as described earlier with CYP2J cDNA as the template, except that the annealing step was carried out at 55°C. The forward primers used were dCYP2J2 (5exp1) 5′-CGCATTAATGGCTCTGTTATTAGCAGTTTTTGCGGCCACCCTCTGGGCAGT-3′ for dog CYP2J2, fCYP2J2 (5exp1a) 5′-GGAATTCCATATGGCTCTGTTATTAGCAGTTTTTGCGGCCGCCGTCTGG-3′ for cat CYP2J2, pCYP2J33 (5exp1) 5′-CGCATTAATGGCTCTGTTATTAGCAGTTTTTGCAGAGGCTCTCTGGAC-3′ for pCYP2J33, pCYP2J34/93 (5exp1) 5′-GGAATTCCATATGGCTCTGTTATTAGCAGTTTTTGCTGAGGCTCTCTGGAC-3′ for pCYP2J34 and pCYP2J93, pCYP2J35 (5exp1) 5′-GGAATTCCATATGGCTCTGTTATTAGCAGTTTTTGCAGAGGTTTTCGGGAC-3′ for pCYP2J35, and pCYP2J2L (5exp1)

DMD Fast Forward. Published on June 14, 2022 as DOI: 10.1124/dmd.122.000930
This article has not been copyedited and formatted. The final version may differ from this version.

5′-GGAATTCCATATGGCTCTGTTATTAGCAGTTTTTGCGGAGGTTCTCTGCAC-3′ for pCYP2J91. The reverse primers were dCYP2J2 (3exp1a) 5′-GCTCTAGACTCTCCTTCAGGACCGAGGGATTGC-3′ for dog CYP2J2, fCYP2J2 (3exp1a) 5′-GCTCTAGACTTCAAGACCGAGGGACTGC-3′ for cat CYP2J2, and pCYP2Js (3exp1a) 5′-GCTCTAGA-CCACAACCTCATGCCCT-3′ for all pig CYP2Js. The forward and reverse primers contained the *Nde*I and *Xba*I sites (underlined), respectively, which were utilized for subcloning into the pCW vector containing human NADPH-P450 reductase cDNA. For dog CYP2J2 and pig CYP2J33, the forward primers contained the *Ase*I site, which generates compatible overhangs for the *Nde*I site. Membrane preparation was performed as described previously (Iwata et al., 1998; Uno et al., 2006). The concentrations of proteins in membrane preparations were determined as previously described for the CYP2J protein (Omura and Sato, 1964) and NAPDH-P450 reductase (Phillips and Langdon, 1962; Iwata et al., 1998).

Measurement of Drug-metabolizing Activities

The activities of recombinant proteins and liver microsomes for terfenadine *t*-butyl hydroxylation, ebastine primary hydroxylation and secondary carebastine formation, and astemizole *O*-demethylation were determined using high-performance liquid chromatography with an ultraviolet detector system with a reversed-phase C_{18} column (5 μm, 150 × 4.6 mm) as described previously (Uehara et al., 2014; Uehara et al., 2015; Uehara et al., 2016; Uehara et al., 2018). Briefly, the incubation mixtures consisted of liver microsomes (0.10 mg/mL) or recombinant CYP2J proteins (20 pmol equivalent/mL), 100 mM potassium phosphate buffer (pH 7.4), an NADPH-generating system (0.25 mM $NADP^+$, 2.5 mM glucose 6-phosphate, and 1 unit/ml glucose-6-phosphate dehydrogenase), and substrate (1.0–100 μM of ebastine or astemizole, 10 μM terfenadine) in a final volume of 0.25 mL. After incubation at 37°C for 10–30 min, reactions were terminated by the addition of 0.25 ml of ice-cold acetonitrile. After centrifugation at 900 × *g* for 5 min, the supernatant was analyzed. Kinetic parameters were calculated from a curve based on Michaelis–Menten or Hill equations fitted by nonlinear regression (mean ± standard error) using Prism (GraphPad Software, La Jolla, CA).

Results

Identification of CYP2J cDNAs

The following CYP2J cDNAs were successfully isolated by RT-PCR using the gene-specific primers designed based on the *CYP2J* gene sequences found in the genomes by BLAT: dog and cat CYP2J2 from liver and pig CYP2J33, CYP2J34, CYP2J35, CYP2J91, and CYP2J93 from liver/small intestine. These CYP2Js were named by the P450 Nomenclature Committee (Nelson, 2009) and had an open reading frame of 502 amino acid residues, except for pig CYP2J35, which had 498 residues. The primary sequence structures were characteristic of P450 proteins, i.e., the presence of six substrate recognition sites (SRSs) (Gotoh, 1992) and a heme-binding region (**Fig. 1**). The amino acid sequences deduced from the CYP2J cDNAs were highly identical (77–80%) to human CYP2J2 (**Table 1**). Phylogenetic analysis of the CYP2J amino acid sequences from humans, cynomolgus macaques, marmosets, pigs, dogs, cats, rats, and mice revealed CYP2J clusters for primates, pigs, dogs/cats, and rats/mice (**Fig. 2**). The CYP2J cDNA sequences identified in the current study were deposited in GenBank under the accession numbers ON164796, ON164791, ON164801, ON164802, ON164803, ON164800, and ON164804 for cat CYP2J2; dog CYP2J2; and pig CYP2J33, CYP2J34, CYP2J35, CYP2J91, and CYP2J93, respectively.

Genome and Gene Structure

The genomic locations of the newly identified *CYP2J* genes were analyzed for dog, cat, pig, and human genome data using BLAT and Sequence Viewer. The analysis indicated that the *CYP2J* gene(s) had the same directions and were in the same locations in the genomes of these species, and six pig *CYP2J* genes (including one pseudogene LOC100525291) formed a gene cluster (**Fig. 3)**. Gene structures were similar among the dog, cat, pig, and human *CYP2J*s. Dog, cat, and human *CYP2J2* genes were approximately 42.0, 31.5, and 33.1 kb, respectively. Among the pig *CYP2J* genes, the largest was *CYP2J91* (>35.6 kb) and the smallest was *CYP2J35* (~23.7 kb). The exon sizes were well conserved in all these *CYP2J* genes (**Fig. 4**), i.e., 163, 150, 161, 177, 142, 188, and 139 bp for exons

2–8, respectively, except for exon 2 (157 bp) and exon 6 (136 bp) of pig *CYP2J35*, which resulted in six amino acids residues fewer than the other CYP2Js. All dog, cat, pig, and human *CYP2J* genes begin with the dinucleotide GU and end with AG, consistent with the consensus sequences for splice junctions in eukaryotic genes.

Tissue Expression

Expressions of dog, cat, and pig CYP2J mRNAs were evaluated using real-time RT-PCR in nine tissue types for dogs and ten tissue types for cats and pigs. Among the tissue types analyzed, cat CYP2J2 mRNA was predominant in small intestine (duodenum, jejunum, and ileum) with lower expression in liver (**Fig. 5**). A similar expression pattern was observed for dog CYP2J2 mRNA, with most abundant expression in small intestine, followed by kidney and liver (**Fig. 5**). In pigs, all the CYP2J mRNAs (except for CYP2J91) also showed predominant expression in small intestine, with more abundant expression in jejunum than ileum, contrasting with dog and cat CYP2J2 mRNAs, which were more abundant in ileum than jejunum (**Fig. 5**). Among the pig CYP2J mRNAs, CYP2J35 mRNA was the most abundant in small intestine, followed by CYP2J93 and CYP2J33 mRNAs (**Fig. 6**). Pig CYP2J35 mRNA was also the most abundant of the pig CYP2J mRNAs in liver, kidney, and lung (**Fig. 6**). In contrast, pig CYP2J91 mRNA was expressed preferentially in brain (**Fig. 5**) and had the highest expression level in brain of all the pig CYP2J mRNAs (**Fig. 6**).

Drug-metabolizing Capabilities of CYP2Js

The drug oxidation activities of recombinant dog CYP2J2; cat CYP2J2; and pig CYP2J33, CYP2J34, CYP2J35, CYP2J91, and CYP2J93 were investigated and compared with those of human CYP2J2. All recombinant dog CYP2J2; cat CYP2J2; and pig CYP2J33, CYP2J34, CYP2J35, CYP2J91, and CYP2J93 showed terfenadine *t*-butyl hydroxylation activities (4-28 nmol/min/nmol CYP2J) roughly comparable with that of human CYP2J2 (20 nmol/min/nmol CYP2J2). The ebastine primary hydroxylation and secondary carebastine formation activities of recombinant CYP2J enzymes were measured at substrate concentrations of 1.0, 10, and 100 μM (**Fig. 7**). Under the present fixed

DMD Fast Forward. Published on June 14, 2022 as DOI: 10.1124/dmd.122.000930
This article has not been copyedited and formatted. The final version may differ from this version.

conditions, human CYP2J2; dog CYP2J2; and pig CYP2J34 and CYP2J35 efficiently oxidized ebastine to the secondary carebastine at low substrate concentrations of 1.0 and 10 μM. The rates of ebastine primary hydroxylation by pig CYP2J33 and CYP2J93 increased with the substrate concentrations, but those by cat CYP2J2 and pig CYP2J91 were apparently saturated at substrate concentrations approaching 10 μM.

Kinetic analyses of astemizole *O*-demethylation using Michaelis–Menten or Hill equations found that for recombinant proteins, the apparent K_m values were in the range of ~1–13 μM, whereas the estimated intrinsic clearance (V_{max}/K_m) values were in the range of ~0.2–1 $\mu M^{-1}min^{-1}$ (**Table 2** and **Fig. 8**). The plots of velocity versus substate concentration exhibited sigmoidal relationships on kinetic analysis of dog CYP2J2, cat CYP2J2, and pig CYP2J33 (**Fig. 8**), which indicated an allosteric interaction (apparent positive cooperativity) between astemizole and CYP2J enzymes; data were analyzed using the general allosteric model and the Hill equation. For human liver microsomes, the K_m value of astemizole *O*-demethylation was 4.5 μM, similar to that for human CYP2J2 recombinant protein, suggesting that human CYP2J2 is predominantly involved in astemizole *O*-demethylation in human liver. In contrast, the Hill coefficient (n) values for human, dog, cat, and pig liver microsomes were 2.2, 1.2, 2.8, and 2.3, respectively, for astemizole *O*-demethylation (**Table 2)**. The calculated S_{50} (K_m) and V_{max} values were, respectively, 30 μM and 0.14 nmol/min/mg for dog liver microsomes, 12 μM and 0.11 nmol/min/mg for cat liver microsomes, and 36 μM and 0.31 nmol/min/mg for pig liver microsomes, implying the possible involvement of additional P450 enzymes because of these higher K_m values than those for recombinant CYP2J enzymes. Overall, these results suggest that dog CYP2J2; cat CYP2J2; and pig CYP2J33, CYP2J34, CYP2J35, CYP2J91, and CYP2J93 all exhibit catalytic function toward typical human CYP2J2 probe substrates terfenadine, ebastine, and astemizole.

Discussion

Human CYP2J2 expressed in small intestine is an important drug-metabolizing enzyme in the first-pass metabolism of drugs such as ebastine and astemizole (Hashizume et al., 2002; Matsumoto et al., 2002). In the present study, we found seven novel *CYP2J* genes in the dog, cat, and pig genome (**Fig. 2**), namely, dog CYP2J2; cat CYP2J2; and pig CYP2J33, CYP2J34, CYP2J35, CYP2J91, and CYP2J93, and the corresponding CYP2J cDNAs were identified. These CYP2Js showed high amino acid sequence identities to human CYP2J2 (**Table 1**) and exhibited the primary sequence characteristics of P450s (**Fig. 1**). All the newly discovered *CYP2J* genes contained conserved exon–intron structures (**Fig. 4**) and were located in corresponding genomic regions in humans, dogs, cats, and pigs; moreover, the pig *CYP2J* genes formed a gene cluster (**Fig. 3**). Therefore, the molecular properties of CYP2Js are generally similar in dogs, cats, pigs, and humans.

Dog, cat, and pig CYP2J mRNAs (except for pCYPJ91) were preferentially expressed in small intestine, among the tissue types analyzed, but were also expressed in liver and heart at lower levels (**Fig. 5**). The relatively low levels of dog, cat, and pig CYP2J mRNAs in heart contrasted with human CYP2J mRNA, which is abundant in heart (Wu et al., 1996; Delozier et al., 2007). This discrepancy might be accounted for by the transactivation mechanism(s) of the *CYP2J* genes, which has not been fully investigated even for human *CYP2J2* gene. In humans, *CYP2J2* contains a TATA-less promoter and putative binding sites for transcription factors [specificity protein-1 (Sp-1) and activator protein-1 (AP-1)] near the 5′-flanking region, which might be involved in *CYP2J2* transcription (Murray, 2016). Disrupting one of the SP-1 binding sites by SNP (*2J2*7*) reduces transcription and enzyme activity of human CYP2J2, and has been reported to be associated with the risk of cardiovascular diseases (Xu et al., 2013; Murray, 2016). Five *CYP2J* genes were found in pigs, unlike in dogs, cats, and humans. Multiple copies of *CYP2J* genes have been found in other species, such as mice (Nelson et al., 2004). Among the pig CYP2J mRNAs, CYP2J35 mRNA, followed by CYP2J93 mRNA, was the most abundant in liver, small intestine, kidney, and lung (**Fig. 6**). It would be of great interest to investigate the transactivation mechanism(s) of dog, cat, and pig *CYP2J* genes and the genetic variants at the

upstream region.

In small intestine, dog and cat CYP2J mRNAs were expressed in jejunum and ileum at comparable levels (**Fig. 5**). Similarly, human CYP2J2 protein is expressed in the gastrointestinal tract, including both jejunum and ileum (Zeldin et al., 1997), in contrast to human CYP3A, CYP2C, and CYP2D6 proteins, which are more abundant in the proximal region than the distal region of the small intestine (Paine et al., 2006). Pig CYP2J33, CYP2J35, and CYP2J93 mRNAs were the most profusely expressed mRNAs in jejunum (**Fig. 6**) and were more abundantly expressed in jejunum than ileum (**Fig. 5**). Such abundant expression of CYP2J mRNAs in small intestine suggests roles for CYP2Js in first-pass metabolism in dogs, cats, and pigs, similar to humans. Pig CYP2J91 mRNA was preferentially expressed in brain (**Fig. 5**), where it was the most abundant pig CYP2J mRNA (**Fig. 6**). Similarly, mouse CYP2J8 and CYP2J9 are abundantly expressed in brain (Qu et al., 2001; Graves et al., 2013). Because CYP2Js are involved in the synthesis of epoxyeicosatrienoic acids, which play protective roles in inflammation and vasodilation (Solanki et al., 2018), CYP2Js in brain might play roles in neuroprotective mechanisms. In contrast, a lower expression of CYP2J mRNAs in heart possibly might suggest only the minor protective roles of CYP2Js in this tissue for dogs, cats, and pigs, although further investigation is needed.

Dog and cat CYP2J2 enzymes showed lower activities than human CYP2J2 for ebastine oxidation (**Fig. 7**). Dog CYP2J2 contains the residues A143 and C158, which are different from the T143 and R158 residues of human CYP2J2, and the substitution T143A was also found in cat CYP2J2 (**Fig. 1**). In human *CYP2J2*, the alleles *CYP2J2*2* and *CYP2J2*3* possess the substitutions T143A and R158C, respectively, resulting in decreased enzyme activity (King et al., 2002). The decreased activities of dog and cat CYP2J2 compared with human CYP2J2 might be accounted for by the substitutions T143A and R158C.

Pig CYP2J34 and CYP2J35 enzymes showed activities roughly comparable to those of human CYP2J2 toward all the substrates analyzed, i.e., ebastine and astemizole (**Figs. 7 and 8**). Although, pig CYP2J34 and CYP2J35 showed high ebastine oxidations rates comparable to human CYP2J2 (**Fig.**

7), pig CYP2J33 mediated astemizole *O*-demethylation even more efficiently than human CYP2J2 (**Fig. 8**). Among the pig CYP2Js, CYP2J91 showed the lowest activities toward the substrates analyzed in the present study (**Figs. 7 and 8**). Compared with human CYP2J2, pig CYP2J91 contained the substitution L378M, which is located in SRS-6 (**Fig. 1**). Molecular docking analysis predicted that residues L378 and G486 are important for recognition and positioning of the substrate in the active site of the enzyme (Xia et al., 2014).

Pig CYP2J35 contained 498 amino acid residues, four residues fewer than the other pig CYP2Js, resulting in substitutions or deletions of four residues in SRS-1 (**Fig. 1**). Of these four residues, the substitution P115L (human *CYP2J2*10* allele) decreases metabolic activity (King et al., 2002), and the residues M116 and R117, among others, play roles in binding and orientation of the substrate in the active site of human CYP2J2, as predicted by molecular docking simulations (Li et al., 2008). The latter study indicated additional residues important for substrate binding and orientation, including F56, L83, G222, L229, I376, G486, L487, and T488, which were found to be substituted in dog, cat, and pig CYP2Js (**Fig. 1**). Some substitutions were located in substrate recognition sites (SRS-1, SRS-4, SRS-5, or SRS-6), which are important for enzyme function (Gotoh, 1992; Lafite et al., 2007; Xu and Chen, 2020); these substitutions included I127V in pig CYP2J33 and CYP2J93, F310V in pig CYP2J93, I376V and I487L in dog CYP2J2, and I487P in all the pig CYP2Js except CYP2J33 (**Fig. 1**). These amino acid substitution(s) likely influence enzyme function, resulting in catalytic activities different from those of human CYP2J2. Taken together, the results of the current study indicated potentially more substantial contributions of pig CYP2J33/34/35 than of pig CYP2J91/93 to CYP2J-dependent drug metabolism in pigs.

In humans, *CYP2J2* exists in various forms, partly due to genetic polymorphisms (Xu et al., 2013; Murray, 2016). Similarly, in dogs, cats, and pigs, genetic variants have been identified, and some of them influence enzyme function (Puccinelli et al., 2011; Martinez et al., 2013; Lee et al., 2019); nonetheless, their relevance to enzyme function largely remains to be determined. It would be of great interest to investigate genetic variants of *CYP2J* in dogs, cats, and pigs.

In conclusion, all seven dog, cat, and pig CYP2Js identified in the present study were highly identical to human CYP2J2 and were functional enzymes able to metabolize the typical human CYP2J2 substrates ebastine, astemizole, and terfenadine. Except for pig CYP2J91 mRNA, all the newly characterized CYP2J mRNAs were expressed predominantly in small intestine, just as human CYP2J2 is. Among the pig CYP2Js investigated, CYP2J93 and CYP2J35 mRNAs were more abundant than other pig CYP2J mRNAs in small intestine, and CYP2J35 showed metabolic properties similar to those of human CYP2J2. Therefore, dog, cat, and pig CYP2Js likely play roles as drug-metabolizing enzymes in small intestine, just as human CYP2J2 does.

Acknowledgments

We thank Drs. Makiko Shimizu and Shotaro Uehara for their assistance. We are also grateful to David Smallbones for copyediting a draft of this article.

Abbreviations

CYP2J, cytochromes P450 2J; P450, cytochrome P450; PCR, polymerase chain reaction; RT, reverse transcription; SRS, substrate recognition site.

Authorship Contributions

Participated in research design: Uno, Yamazaki.

Conducted experiments: Uno, Murayama.

Contributed new reagents or analytic tools: Uno, Ijiri, Kawaguchi, Yamato, Teraoka, Mizukawa, Nakayama, Ikenaka, and Ishizuka.

Performed data analysis: Uno, Asano, Shiraishi, Yamazaki.

Wrote or contributed to the writing of the manuscript: Uno and Yamazaki.

References

Court MH (2013) Canine cytochrome P-450 pharmacogenetics. *Vet Clin North Am Small Anim Pract* **43:**1027-1038.

Delozier TC, Kissling GE, Coulter SJ, Dai D, Foley JF, Bradbury JA, Murphy E, Steenbergen C, Zeldin DC, and Goldstein JA (2007) Detection of human CYP2C8, CYP2C9, and CYP2J2 in cardiovascular tissues. *Drug Metab Dispos* **35:**682-688.

Elmorsi Y, Al Feteisi H, Al-Majdoub ZM, Barber J, Rostami-Hodjegan A, and Achour B (2020) Proteomic characterisation of drug metabolising enzymes and drug transporters in pig liver. *Xenobiotica* **50:**1208-1219.

Gotoh O (1992) Substrate recognition sites in cytochrome P450 family 2 (CYP2) proteins inferred from comparative analyses of amino acid and coding nucleotide sequences. *J Biol Chem* **267:**83-90.

Graves JP, Edin ML, Bradbury JA, Gruzdev A, Cheng J, Lih FB, Masinde TA, Qu W, Clayton NP, Morrison JP, Tomer KB, and Zeldin DC (2013) Characterization of four new mouse cytochrome P450 enzymes of the CYP2J subfamily. *Drug Metab Dispos* **41:**763-773.

Hashizume T, Imaoka S, Mise M, Terauchi Y, Fujii T, Miyazaki H, Kamataki T, and Funae Y (2002) Involvement of CYP2J2 and CYP4F12 in the metabolism of ebastine in human intestinal microsomes. *J Pharmacol Exp Ther* **300:**298-304.

Iwata H, Fujita K, Kushida H, Suzuki A, Konno Y, Nakamura K, Fujino A, and Kamataki T (1998) High catalytic activity of human cytochrome P450 co-expressed with human NADPH-cytochrome P450 reductase in Escherichia coli. *Biochem Pharmacol* **55:**1315-1325.

King LM, Ma J, Srettabunjong S, Graves J, Bradbury JA, Li L, Spiecker M, Liao JK, Mohrenweiser H, and Zeldin DC (2002) Cloning of CYP2J2 gene and identification of functional polymorphisms. *Mol Pharmacol* **61:**840-852.

Lafite P, Andre F, Zeldin DC, Dansette PM, and Mansuy D (2007) Unusual regioselectivity and active site topology of human cytochrome P450 2J2. *Biochemistry* **46:**10237-10247.

Lee CA, Neul D, Clouser-Roche A, Dalvie D, Wester MR, Jiang Y, Jones III JP, Freiwald S, Zientek M, and Totah RA (2010) Identification of novel substrates for human cytochrome P450 2J2. *Drug Metab Dispos* **38:**347-356.

Lee PM, Faus MCL, and Court MH (2019) High interindividual variability in plasma clopidogrel active metabolite concentrations in healthy cats is associated with sex and cytochrome P450 2C genetic polymorphism. *J Vet Pharmacol Ther* **42:**16-25.

Li W, Tang Y, Liu H, Cheng J, Zhu W, and Jiang H (2008) Probing ligand binding modes of human cytochrome P450 2J2 by homology modeling, molecular dynamics simulation, and flexible molecular docking. *Proteins* **71:**938-949.

Martinez MN, Antonovic L, Court M, Dacasto M, Fink-Gremmels J, Kukanich B, Locuson C, Mealey K, Myers MJ, and Trepanier L (2013) Challenges in exploring the cytochrome P450 system as a source of variation in canine drug pharmacokinetics. *Drug Metab Rev* **45:**218-230.

Matsumoto S, Hirama T, Matsubara T, Nagata K, and Yamazoe Y (2002) Involvement of CYP2J2 on the intestinal first-pass metabolism of antihistamine drug, astemizole. *Drug Metab Dispos* **30:**1240-1245.

Murray M (2016) CYP2J2 – regulation, function and polymorphism. *Drug Metab Rev* **48:**351-368.

Nelson DR (2009) The cytochrome p450 homepage. *Hum Genomics* **4:**59-65.

Nelson DR, Zeldin DC, Hoffman SM, Maltais LJ, Wain HM, and Nebert DW (2004) Comparison of cytochrome P450 (CYP) genes from the mouse and human genomes, including nomenclature recommendations for genes, pseudogenes and alternative-splice variants. *Pharmacogenetics* **14:**1-18.

Omura T and Sato R (1964) The carbon monoxide-binding pigment of liver microsomes. I. Evidence for its hemoprotein nature. *J Biol Chem* **239:**2370-2378.

Ono Y, Sugiyama S, Matsushita M, Kitazawa T, Amano T, Uno Y, Ikushiro S, and Teraoka H (2019) Limited expression of functional cytochrome p450 2c subtypes in the liver and small intestine of domestic cats. *Xenobiotica* **49:**627-635.

Paine MF, Hart HL, Ludington SS, Haining RL, Rettie AE, and Zeldin DC (2006) The human intestinal cytochrome P450 "pie". *Drug Metab Dispos* **34:**880-886.

Phillips AH and Langdon RG (1962) Hepatic triphosphopyridine nucleotide-cytochrome c reductase: isolation, characterization, and kinetic studies. *J Biol Chem* **237:**2652-2660.

Puccinelli E, Gervasi PG, and Longo V (2011) Xenobiotic metabolizing cytochrome P450 in pig, a promising animal model. *Curr Drug Metab* **12:**507-525.

Qu W, Bradbury JA, Tsao CC, Maronpot R, Harry GJ, Parker CE, Davis LS, Breyer MD, Waalkes MP, Falck JR, Chen J, Rosenberg RL, and Zeldin DC (2001) Cytochrome P450 CYP2J9, a new mouse arachidonic acid omega-1 hydroxylase predominantly expressed in brain. *J Biol Chem* **276:**25467-25479.

Solanki M, Pointon A, Jones B, and Herbert K (2018) Cytochrome P450 2J2: potential role in drug metabolism and cardiotoxicity. *Drug Metab Dispos* **46:**1053-1065.

Uehara S, Murayama N, Nakanishi Y, Nakamura C, Hashizume T, Zeldin DC, Yamazaki H, and Uno Y (2014) Immunochemical detection of cytochrome P450 enzymes in small intestine microsomes of male and female untreated juvenile cynomolgus monkeys. *Xenobiotica* **44:**769-774.

Uehara S, Murayama N, Nakanishi Y, Nakamura C, Hashizume T, Zeldin DC, Yamazaki H, and Uno Y (2015) Immunochemical quantification of cynomolgus CYP2J2, CYP4A and CYP4F enzymes in liver and small intestine. *Xenobiotica* **45:**124-130.

Uehara S, Uno Y, Inoue T, Okamoto E, Sasaki E, and Yamazaki H (2016) Marmoset cytochrome P450 2J2 mainly expressed in small intestines and livers effectively metabolizes human P450 2J2 probe substrates, astemizole and terfenadine. *Xenobiotica* **46:**977-985.

Uehara S, Yuki Y, Uno Y, Inoue T, Sasaki E, and Yamazaki H (2018) Terfenadine t-butyl hydroxylation catalyzed by human and marmoset cytochrome P450 3A and 4F enzymes in livers and small intestines. *Xenobiotica* **48:**342-347.

Uno Y, Fujino H, Kito G, Kamataki T, and Nagata R (2006) CYP2C76, a novel cytochrome P450 in cynomolgus monkey, is a major CYP2C in liver, metabolizing tolbutamide and testosterone. *Mol Pharmacol* **70:**477-486.

Wu S, Moomaw CR, Tomer KB, Falck JR, and Zeldin DC (1996) Molecular cloning and expression of CYP2J2, a human cytochrome P450 arachidonic acid epoxygenase highly expressed in heart. *J Biol Chem* **271:**3460-3468.

Xia XL, Fa BT, Cong S, Wang JF, and Chou KC (2014) Research/review: Insights into the mutation-induced dysfunction of arachidonic acid metabolism from modeling of human CYP2J2. *Curr Drug Metab* **15:**502-513.

Xu L and Chen LY (2020) Molecular determinant of substrate binding and specificity of cytochrome P450 2J2. *Sci Rep* **10:**22267.

Xu M, Ju W, Hao H, Wang G, and Li P (2013) Cytochrome P450 2J2: distribution, function, regulation, genetic polymorphisms and clinical significance. *Drug Metab Rev* **45:**311-352.

Zeldin DC, Foley J, Goldsworthy SM, Cook ME, Boyle JE, Ma J, Moomaw CR, Tomer KB, Steenbergen C, and Wu S (1997) CYP2J subfamily cytochrome P450s in the gastrointestinal tract: expression, localization, and potential functional significance. *Mol Pharmacol* **51:**931-943.

Footnotes

Funding

This work was supported partly by the Japan Society for the Promotion of Science Grant-in-Aid for Scientific Research 20K06434.

Declaration of Interest

The authors have no competing interests to declare.

DMD Fast Forward. Published on June 14, 2022 as DOI: 10.1124/dmd.122.000930
This article has not been copyedited and formatted. The final version may differ from this version.

Figure Legends

Fig. 1. Amino acid sequences deduced from dog, cat, and pig CYP2J cDNAs. Amino acid sequences of dog (d), cat (f), pig (p), and human (h) CYP2Js were aligned using ClustalW program. The broken line above the sequences indicates the putative heme-binding region characteristic of P450 protein, and the solid lines show the six putative substrate recognition sites (SRSs). Asterisks and dots under the sequences indicate identical amino acids and conservatively changed amino acids, respectively.

Fig. 2. Phylogenetic tree of CYP2J amino acid sequences created using the neighbor-joining method for CYP2J amino acid sequences from humans (h), cynomolgus macaques (mf), marmosets (cj), dogs (d), cats (f), pigs (p), rats (r), and mice (m). The scale bar indicates 0.1 amino acid substitutions per site for distance measurement. Chicken (ck) CYP2J23 was used as the outgroup.

Fig. 3. Genomic structure of *CYP2J* genes. The dog, cat, pig, and human genomes were analyzed using BLAT and Sequence Viewer. The pig *CYP2J* genes formed a gene cluster in the genome, unlike cat, dog, or human *CYP2J2*. The locations in the genome and directions of these *CYP2J* genes were similar among dogs, cats, pigs, and humans. Black and gray arrows, respectively, indicate functional and pseudogenized *CYP2J* genes, while white arrows show non-*CYP2J* genes. The sizes of the genes and the distances between them are not proportional to actual measurements.

Fig. 4. Gene structures of *CYP2J* genes. The coding region of each CYP2J cDNA sequence was aligned with the genome using BLAT to determine the gene structures for dog (d), cat (f), pig (p), and human (h) *CYP2J* genes.

Fig. 5. Tissue expression patterns of CYP2J mRNAs. The expression levels of dog, cat, and pig CYP2J mRNAs were measured using real-time RT-PCR in adrenal gland, brain, duodenum, heart, ileum, jejunum, liver, lung, kidney, ovary, spleen, and testis/uterus. Expression levels of each CYP2J mRNA were normalized using the expression level of 18S rRNA and represent the average ± S.D. from three independent amplifications. The most abundant expression level was arbitrarily set to 1, and all other expression levels were adjusted accordingly.

Fig. 6. Expression levels of pig CYP2J mRNAs in brain, jejunum, kidney, liver, lung, and heart. Averaged quantitative values of expression levels were compared among pig CYP2J mRNAs in brain, jejunum, kidney, liver, lung, and heart. Pig CYP2J35 mRNA was most abundantly expressed in liver, kidney, jejunum, and lung, although pig CYP2J93 mRNA was also abundantly expressed in jejunum. The most abundant expression was arbitrarily set to 1, to which all other values were adjusted.

Fig. 7. Ebastine oxidation by recombinant P450 2J proteins. Ebastine primary hydroxylation (white) and secondary carebastine formation (gray) by recombinant human (A), dog (B), cat (C), and pig CYP2J proteins (D–H) at substrate concentrations of 1, 10, and 100 μM were determined at 37°C for 10 min.

Fig. 8. Astemizole *O*-demethylation by recombinant CYP2J proteins (A–D) and liver microsomes (E–H) from humans, dogs, cats, and pigs. The kinetic parameters under the present conditions are shown in **Table 2**.

Table 1

Sequence identities of dog, cat, and pig CYP2Js compared with human CYP2J2

P450	cDNA (%)	Amino acids (%)
Dog CYP2J2	85	79
Cat CYP2J2	85	80
Pig CYP2J33	84	77
Pig CYP2J34	83	78
Pig CYP2J35	83	77
Pig CYP2J91	84	80
Pig CYP2J93	83	78

Dog, cat, and pig CYP2J amino acid and cDNA sequences (coding region) were compared using BLAST.

DMD Fast Forward. Published on June 14, 2022 as DOI: 10.1124/dmd.122.000930
This article has not been copyedited and formatted. The final version may differ from this version.

Table 2

Kinetic parameters of astemizole *O*-demethylation by recombinant CYP2J enzymes and liver microsomes

Enzyme source	K_m or S_{50}	Hill coefficient	V_{max}	V_{max}/K_m (S_{50})
Recombinant P450	(μM)		(min^{-1})	(mL/min/nmol)
Human CYP2J2	6.5 ± 0.7		3.3 ± 0.1	0.51
Dog CYP2J2	5.7 ± 1.0	2.5 ± 0.9	5.8 ± 0.3	1.0
Cat CYP2J2	3.3 ± 0.5	2.8 ± 1.1	2.6 ± 0.2	0.79
Pig CYP2J33	13 ± 1	1.7 ± 0.1	8.5 ± 0.3	0.65
Pig CYP2J34	5.3 ± 2.1		1.6 ± 0.2	0.30
Pig CYP2J35	8.8 ± 2.2		3.0 ± 0.2	0.34
Pig CYP2J91	0.82 ± 0.12		0.49 ± 0.01	0.60
Pig CYP2J93	2.0 ± 0.5		0.33 ± 0.01	0.17
Liver microsomes			(nmol/min/mg)	(μL/min/mg)
Human	4.5 ± 0.4	2.2 ± 0.3	0.15 ± 0.01	33
Dog	30 ± 9	1.2 ± 0.2	0.14 ± 0.02	4.7
Cat	12 ± 1	2.8 ± 0.6	0.11 ± 0.01	9.2
Pig	36 ± 7	2.3 ± 0.7	0.31 ± 0.05	8.6

Kinetic parameters were calculated by nonlinear regression analysis (mean ± standard error, n = 12 substrate concentrations in the range 1.0–100 μM)

DMD Fast Forward. Published on June 14, 2022 as DOI: 10.1124/dmd.122.000930
This article has not been copyedited and formatted. The final version may differ from this version.

Fig. 1

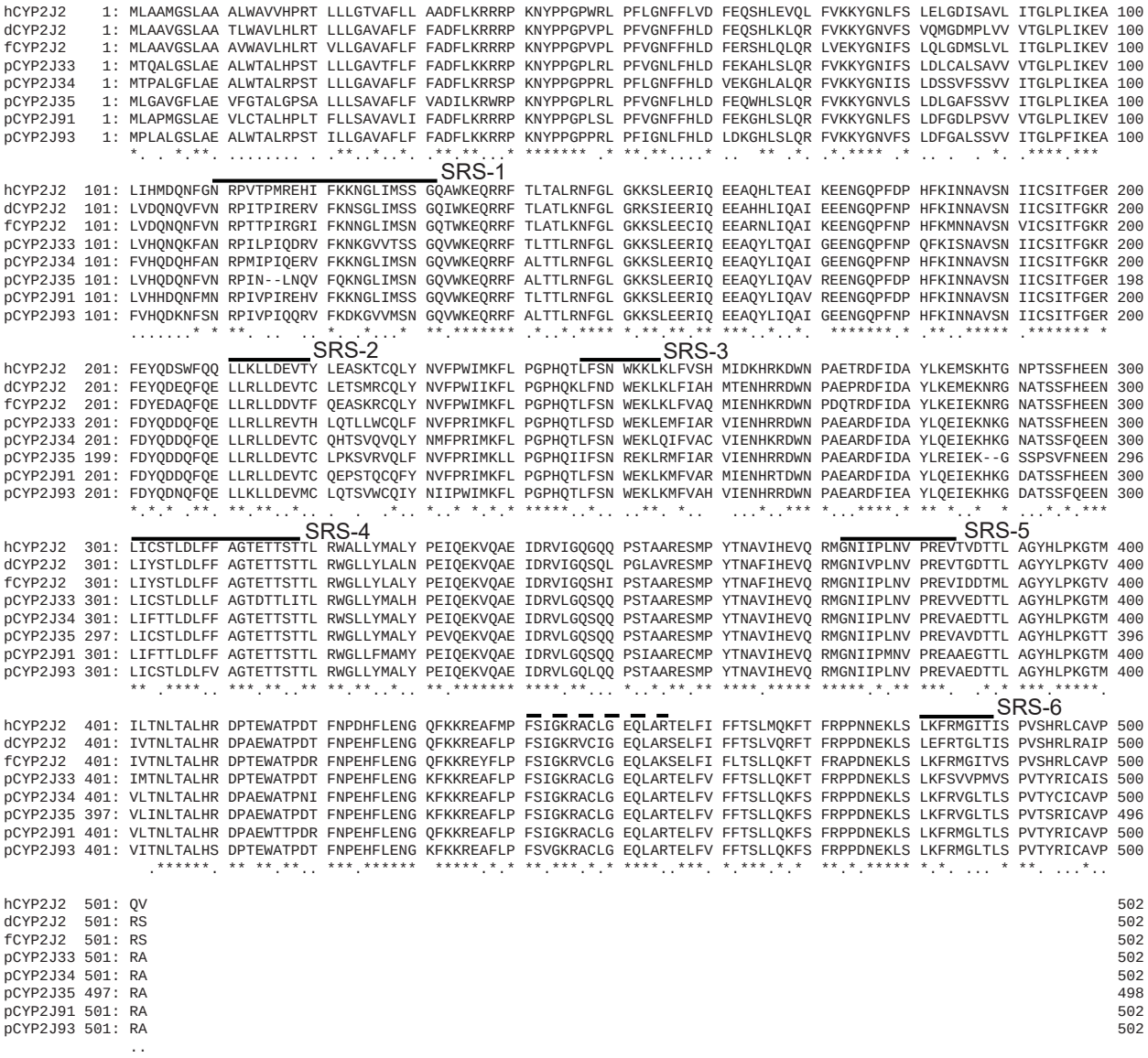

DMD Fast Forward. Published on June 14, 2022 as DOI: 10.1124/dmd.122.000930
This article has not been copyedited and formatted. The final version may differ from this version.

Fig. 2

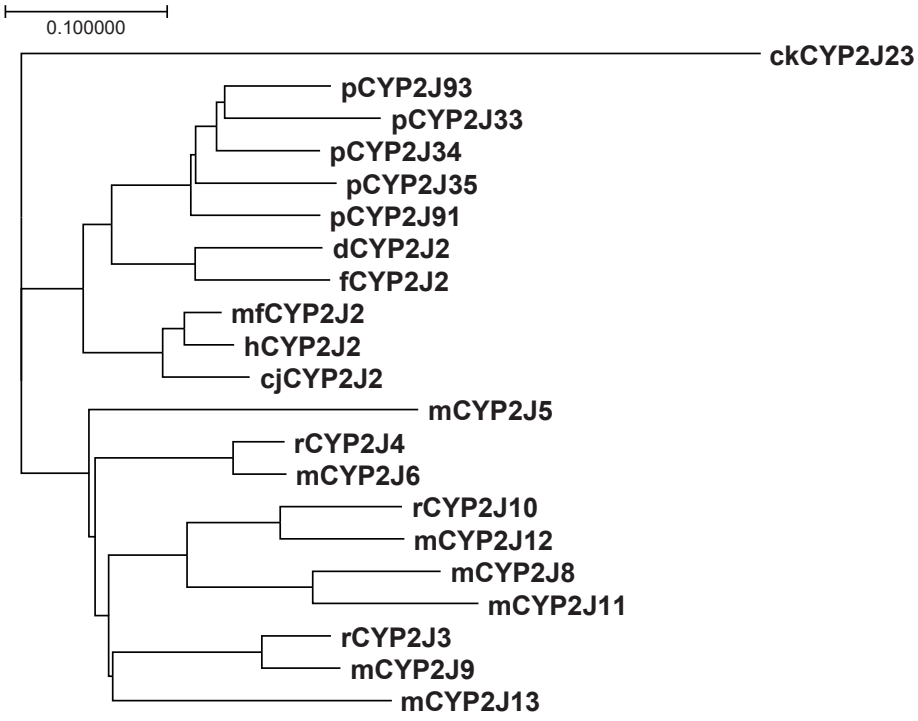

Fig. 3

DMD Fast Forward. Published on June 14, 2022 as DOI: 10.1124/dmd.122.000930
This article has not been copyedited and formatted. The final version may differ from this version.

Human chromosome 1
Dog chromosome 5
Cat chromosome C1

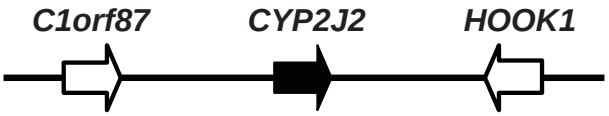

Pig chromosome 4

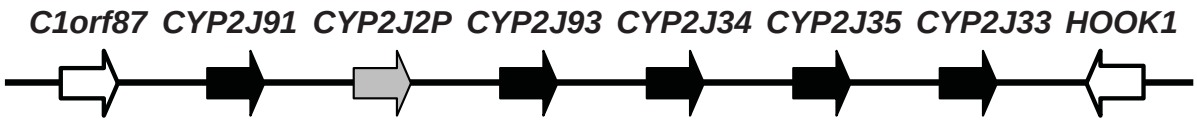

DMD Fast Forward. Published on June 14, 2022 as DOI: 10.1124/dmd.122.000930
This article has not been copyedited and formatted. The final version may differ from this version.

Fig. 4

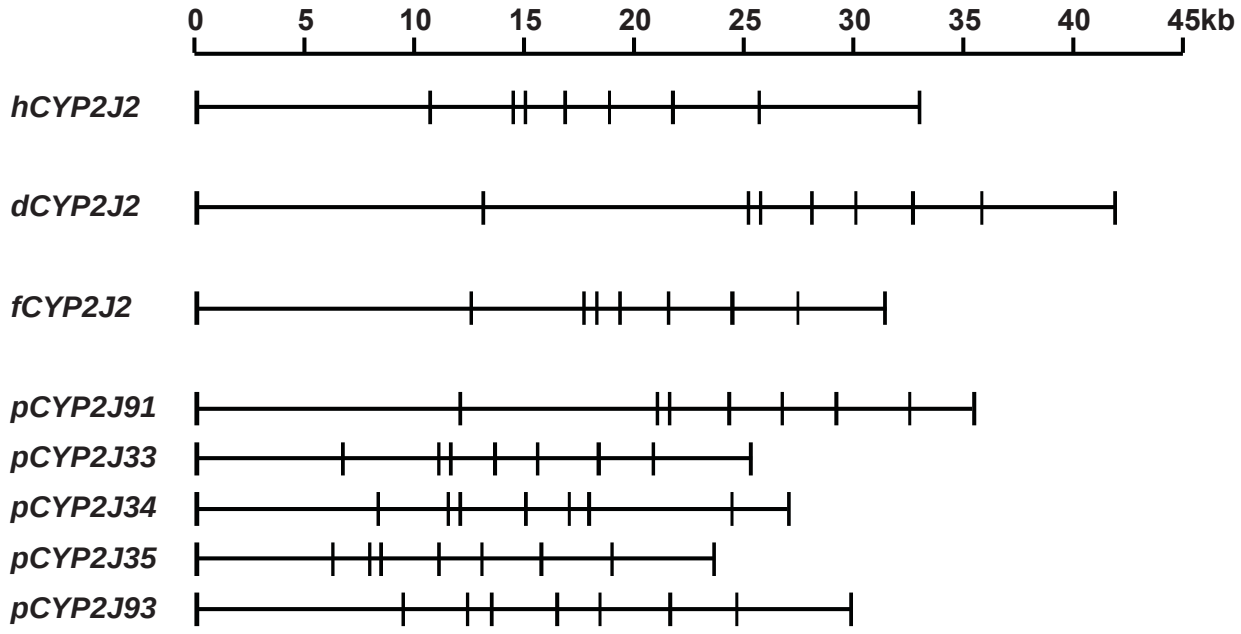

DMD Fast Forward. Published on June 14, 2022 as DOI: 10.1124/dmd.122.000930
This article has not been copyedited and formatted. The final version may differ from this version.

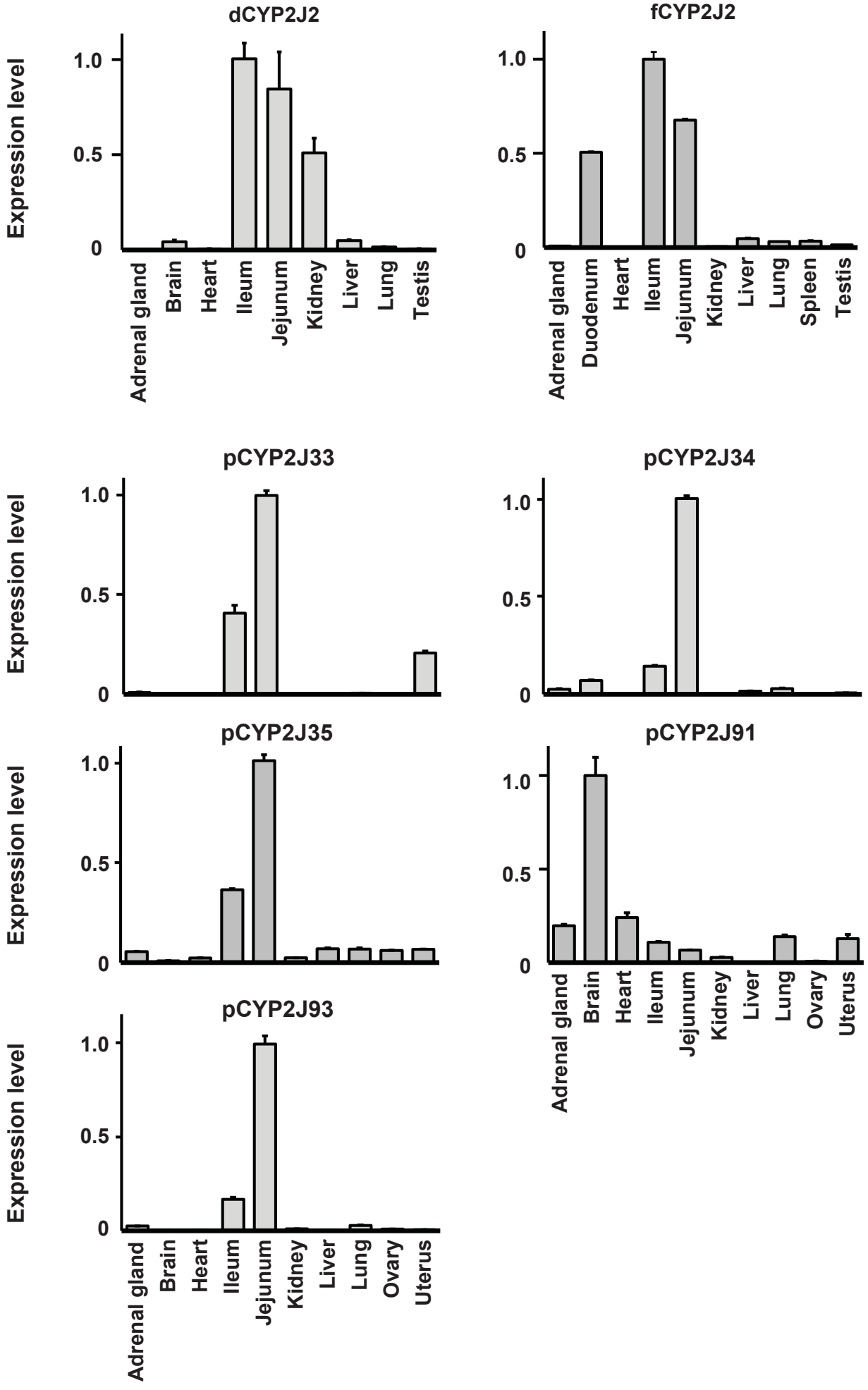

Fig. 6

DMD Fast Forward. Published on June 14, 2022 as DOI: 10.1124/dmd.122.000930
This article has not been copyedited and formatted. The final version may differ from this version.

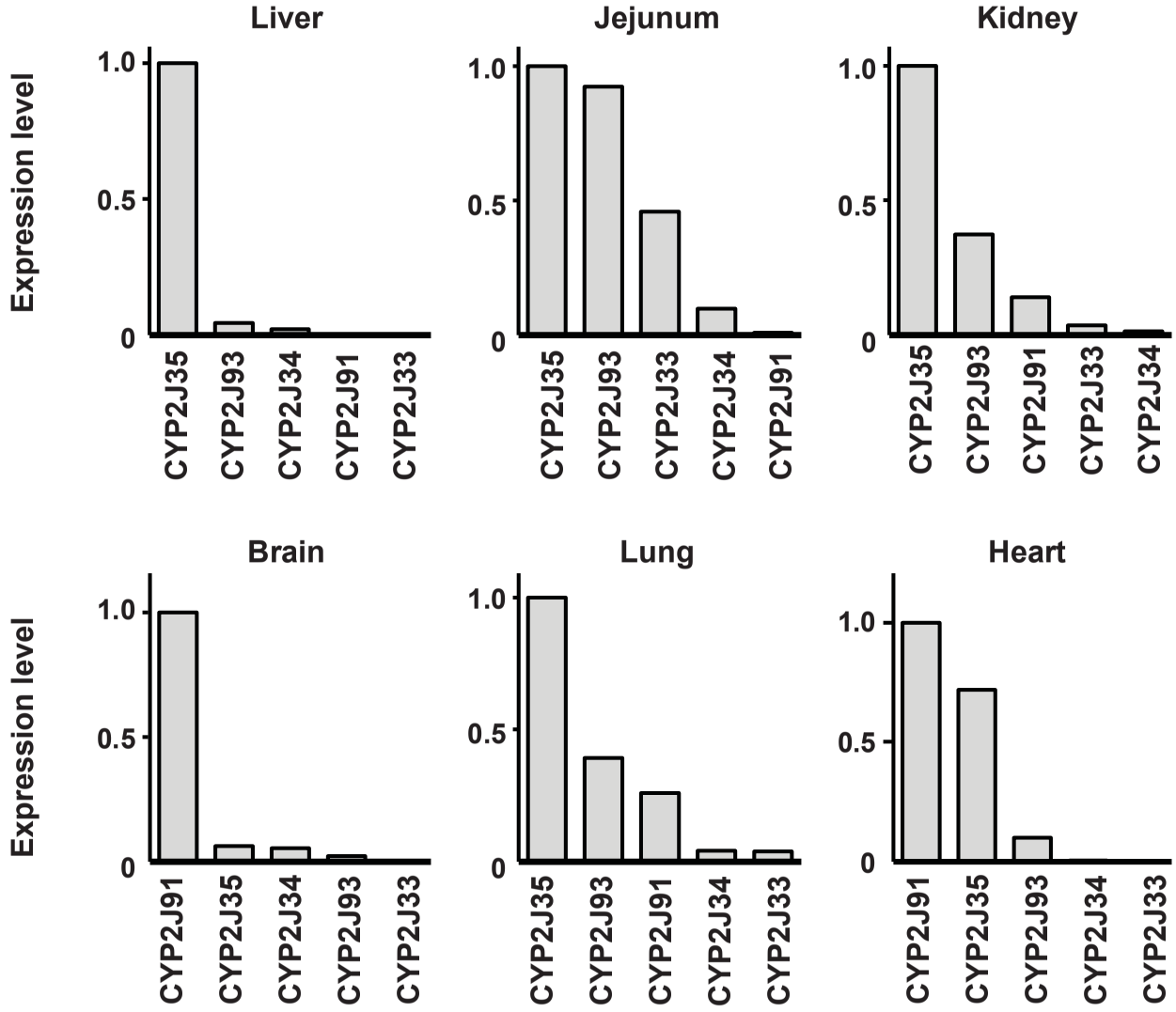

Fig. 7

DMD Fast Forward. Published on June 14, 2022 as DOI: 10.1124/dmd.122.000930
This article has not been copyedited and formatted. The final version may differ from this version.

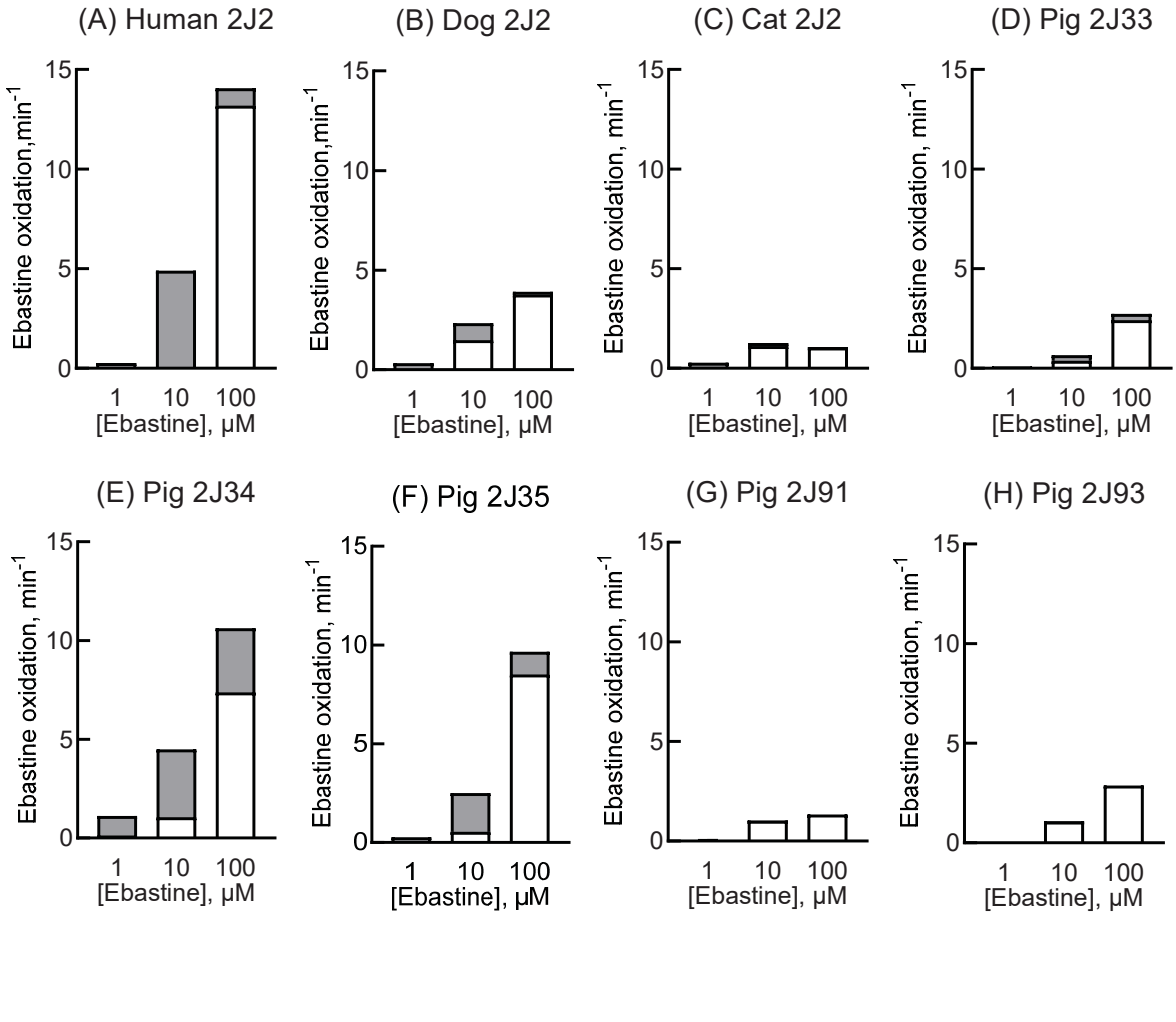

DMD Fast Forward. Published on June 14, 2022 as DOI: 10.1124/dmd.122.000930
This article has not been copyedited and formatted. The final version may differ from this version.

Fig. 8